InAs/AlSb/GaSb singlebarrier interband tunneling diodes with high peaktovalley ratios at room temperature

J. F. Chen, M. C. Wu, L. Yang, and A. Y. Cho

Articles you may be interested in

Improvement of peaktovalley ratio by the incorporation of the InAs layer into the GaSb/AlSb/GaSb/AlSb/InAs double barrier resonant interband tunneling structure
Appl. Phys. Lett. **60**, 713 (1992); 10.1063/1.106546

Highly strained GaAs/InGaAs/AlAs resonant tunneling diodes with simultaneously high peak current densities and peaktovalley ratios at room temperature
Appl. Phys. Lett. **58**, 2255 (1991); 10.1063/1.104943

On the effect of the barrier widths in the InAs/AlSb/GaSb singlebarrier interband tunneling structures
J. Appl. Phys. **68**, 3451 (1990); 10.1063/1.346355

Interband tunneling in singlebarrier InAs/AlSb/GaSb heterostructures
Appl. Phys. Lett. **56**, 952 (1990); 10.1063/1.102634

Demonstration of large peaktovalley current ratios in InAs/AlGaSb/InAs singlebarrier heterostructures
Appl. Phys. Lett. **55**, 1348 (1989); 10.1063/1.101595

---

[1] Y. Shiraki, Y. Katayama, Y. Kobayashi, and K. F. Komatsubara, J. Cryst. Growth 45, 278 (1978).
[2] E. Kasper and H. J. Herzog, Wiss. Ber. Allg. Elektricitaets Ges. Telefunken 49, 213 (1976).
[3] B. Y. Tsauer, M. W. Geis, and J. C. C. Fan, Appl. Phys. Lett. 38, 779 (1981).
[4] K. Ishibashi and S. Furukawa, IEEE Trans. Electron Devices ED-33, 322 (1986).
[5] A. Ishizaka and Shiraki, J. Electrochem. Soc. 33, 666 (1986).
[6] K. Kugimiya, Y. Hirofuji, and N. Matsuo, Jpn. J. Appl. Phys. 24, 564 (1985).
[7] K. C. Prince, U. Breuer, and P. Bonzel, Phys. Rev. Lett. 60, 1146 (1988).
[8] E. G. McRae and R. A. Malic, Phys. Rev. Lett. 58, 1437 (1887).
[9] M. Marurama, J. Crist. Growth 94, 757 (1989).
[10] M. Ichikawa, Mater. Sci. Rep. 4(4), 147 (1989).
[11] U. Kohler, J. Vac. Sci. Technol. A 7, 2860 (1989).
[12] J. Villain, D. R. Grempel, and J. Lapujoulade, J. Phys. F 15, 809 (1985).

InAs/AlSb/GaSb single-barrier interband tunneling diodes with high peak-to-valley ratios at room temperature

J. F. Chen, M. C. Wu, L. Yang, and A. Y. Cho
AT&T Bell Laboratories, Murray Hill, New Jersey 07974

We have fabricated an InAs/AlSb/GaSb single-barrier interband tunneling diode by molecular beam epitaxy. In this structure, a large tunneling current can be obtained by taking the advantage of the large heterojunction-conduction band to valence band overlap (0.15 eV) between InAs and GaSb which offers flexible designs of the AlSb barrier thickness and the doping concentrations. We have obtained a negative differential resistance with a peak-to-valley current ratio as high as 4.7 and a peak current density of 3.5 kA/cm^2 at room temperature with a 1.5-nm-thick AlSb barrier. The current transport mechanism in this tunneling structure will be discussed according to the *I-V* characteristics as a function of temperature.

Since the discovery of the negative resistance in the tunnel diodes (Esaki diodes),[1] they have been extensively studied due to their applications in microwave and high-speed digital circuits. The physical basis of a *pn*-tunnel diode is the interband tunneling, from the conduction band into the valence band and vice versa. Negative resistance can also result from resonant tunneling,[2] where electrons tunnel through a quasibound state of a quantum well. There has been a growing interest in the development of resonant tunneling diodes owing to the rapid advances in semiconductor growth technology, such as molecular beam epitaxy (MBE) that makes it possible to control the composition and doping of the grown material on an atomic scale.[3] Most of the resonant tunneling structures were studied in the AlGaAs/GaAs (Ref. 4) or InGaAs/InAlAs (Ref. 5) material system.

Recently, the AlSb/GaSb/InAs material system was used in tunneling applications[6–10] due to its unique band alignment. For example, AlSb/InAs provides a large barrier for electrons (1.8 eV),[11] which is expected to provide high peak-to-valley ratio (PVR) in double barrier diodes. Perhaps the most interesting feature in this material system is that the conduction band of InAs is 0.15 eV (Ref. 12) lower in energy than the valence band of GaSb. The electrons can flow from the conduction band of the InAs to the valence band of the GaSb. By using AlSb as a barrier layer

between the InAs and the GaSb, a negative resistance similar to homojunction *pn*-tunnel diode can be obtained. However, in a homojunction tunnel diode, degenerate doping is required to make the tunneling barrier thin enough to obtain significant interband tunneling. In the InAs/AlSb/GaSb structure, the interband tunneling is provided by the band overlap between the InAs and the GaSb. This relatively large band overlap will provide a large tunneling-current flow. With the optimal control in design parameters such as the thickness of the AlSb barrier and the growth conditions, a large PVR and a large peak-current density can be realized. It should be noted that this structure offers a flexible design in device parameters, such as independent control of the barrier thickness and doping concentrations. The interband tunneling based on the InAs/AlSb/GaSb material system was first demonstrated by Takaoka *et al.*[13] Recently, Luo *et al.*[14] report their experimental measurements of a InAs/AlSb/GaSb interband tunneling. A peak-to-valley ratio of 2.7:1 and a peak current density of 10 A/cm^2 at 77 K was reported in their case. In this communication, we report on the room-temperature operation (PVR = 4.7 and a peak-current density = 3.5 kA/cm^2) of the InAs/AlSb/GaSb single-barrier interband tunneling diode and their current-voltage-temperature characteristics.

Figure 1 shows the band diagrams of a single-barrier

InAs-AlSb-GaSb heterostructure under different bias conditions. The band alignment in this structure was first studied by Esaki et al.[15] The GaSb/AlSb valence-band offset is assumed to be 0.4 eV. The valence band edge of AlSb is assumed to be aligned with that of the InAs for simplicity, since their relative locations are not accurately known at present.[13] The InAs and GaSb form a broken-gap heterojunction, with the conduction band of InAs 0.15 eV lower in energy than the valence band of GaSb. Provided the AlSb barrier is thin enough, the electrons can tunnel from the conduction band of the InAs, through the AlSb barrier into the valence band of the GaSb, as indicated by an arrow directed from left to right in Fig. 1(a). Under a forward bias less than the band overlap, this relatively large band overlap will provide a large tunneling-current flow. Figure 1(b) shows that as the bias is increased, the valence band of GaSb is pushed down below the conduction band of InAs. The electrons of the InAs experience a very thick barrier to tunnel through, thus reducing the interband tunneling current. This current transport mechanism is qualitatively similar to the homojunction pn-tunnel diode. With further increases of the forward bias, tunneling as indicated in Fig. 1(c), or thermionic-tunneling current may begin to dominate.

The epitaxial layer structure of our device shown in Fig. 1 was grown on a S-doped InAs (100) substrate in Riber-2300 MBE system. The system is equipped with a standard As cell producing As tetramers, and a cracked Sb cell producing Sb dimers. The substrate was chemically polished and etched using diluted Bromine-Methanol solution prior to the epitaxial growth. A 0.5-μm-thick InAs buffer layer was grown at a substrate temperature of 400 °C with a growth rate of 0.5 μm/h. The flux ratio of As:In was adjusted to make the reflection high-energy electron (RHEED) pattern show a streaky (1×1) reconstruction. This condition, corresponding to that of intermediate between (2×4) As-stabilized and (4×2) In-stabilized reconstruction, provides good electrical properties.[16] The undoped InAs layers show n-type background concentrations on the order of 5×10^{15} cm^{-3}. With such a growth condition, the grown sample exhibits good surface morphology. After the completion of InAs buffer layer, the substrate temperature was raised to 450–500 °C and the whole diode structure was subsequently grown. The diode structure consisted of a 5-nm undoped-InAs spacer layer, a 1.5 nm undoped-AlSb barrier, a 5-nm undoped-GaSb spacer layer and a 80-nm Be-doped ($2-5 \times 10^{18}$ cm^{-3}) GaSb top layer. Transmission electron microscopy (TEM) measurements showed that the dislocation density around the active region in the grown structure ranged from 10^6 to 10^7 cm^{-2}, which was nearly the same order of density as that of the starting substrate we used. AlSb and GaSb were grown at a growth rate of 0.5 μm/h with beam equivalent pressure (BEP) ratio of Sb to Al or Ga about 3:1. The undoped-
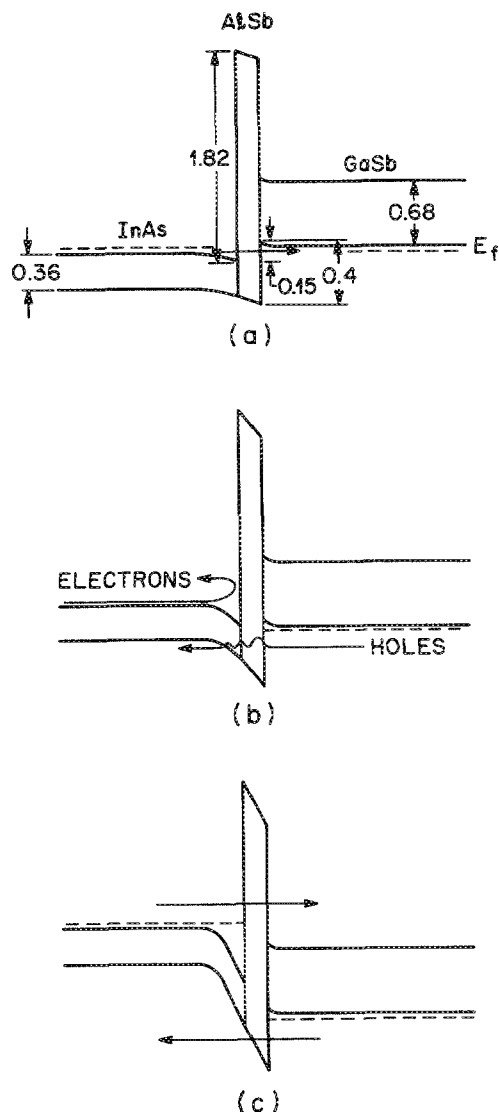

FIG. 1. Energy-band diagram of the InAs/AlSb/GaSb single-barrier interband tunneling diode. (a) At forward bias, the electrons tunnel from the conduction band (CB) of the InAs layer, through the AlSb barrier into the valence band (VB) of the GaSb layer. (b) The bias is increased to the point that the valence band of the GaSb layer is pushed down below the conduction band of the InAs layer. (c) With further increase of the forward bias, the CB-CB (or VB-VB) tunneling current begins to dominate.
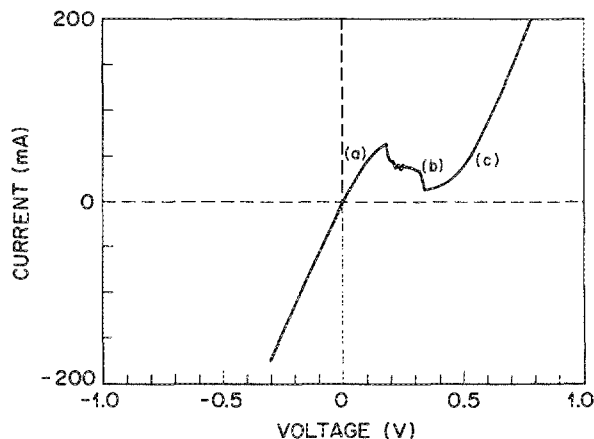

FIG. 2. Current-Voltage characteristic of the single-barrier tunneling diode at room temperature, showing a peak-to-valley current ratio of 4.7.

GaSb layers were found to be p-type with a typical carrier concentration of 10^{16} cm^{-3}. Undoped AlSb has a relatively high resistivity on the order of 10^3 Ω cm. Mesa isolation was formed using chemical etching after alloyed Au/Be contacts were deposited.

Figure 2 shows the room temperature I-V characteristics for the sample with a 1.5-nm-thick AlSb barrier. The current bump in the negative differential resistance (NDR) region results from the circuit oscillation in the testing set-up. Unlike the double-barrier tunneling structure, a negative resistance can only be seen at the forward bias. Under the reverse bias condition, the current is dominated by the electrons tunneling from the valence band of GaSb through the AlSb into the conduction band of the InAs. Designations of (a), (b), and (c) in Fig. 2 correspond to the different forward biases as indicated in Fig. 1. In Fig. 2, a peak-current density of 3.5 kA/cm^2 and a peak-to-valley ratio (PVR) as high as 4.7 at room temperature has been obtained for the diodes with a 60-μm-diam dots. Note that the NDR occurs at about 0.25 V which is relatively low compared with that of the resonant tunneling diode. This low dc operation point reduces the dc power dissipation, when the device is operated in high-speed circuits. After the correction for the probe-contact resistance (typically 1 Ω), the peak current occurs at about 0.12 V. This value is consistent with a band overlap of 0.15 eV between InAs and GaSb.

To study the current transport mechanism in more details, the I-V characteristics as a function of temperature were measured. Figure 3 shows the variations of the forward currents with temperature ranging from 77 to 300 K for several different biases in the tunnel diode. Among the five biases, 100 and 200 mV correspond to the biases below the peak-current voltage. As indicated in Fig. 3, the temperature dependence of currents for these two biases is very weak, suggesting that the current transport is dominated by the tunneling process. This corresponds to the current component that the electrons from the conduction band of
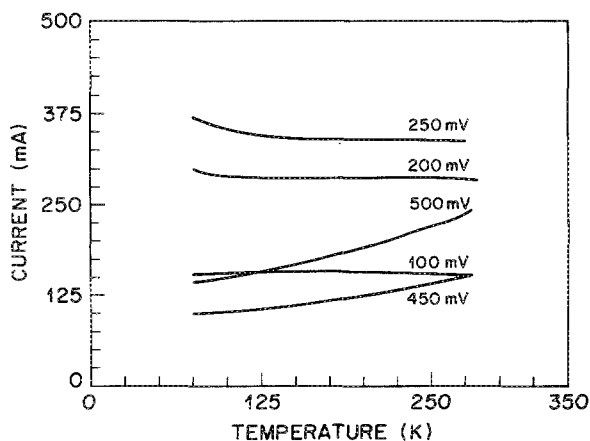
the InAs tunnel through the thin AlSb barrier into the valence band of the GaSb, as indicated in Fig. 1(a). At the bias of 250 mV (close to the peak-current voltage), the current slightly increases with decreasing temperature. This temperature-dependence can be interpreted by the decrease of thermal spreading (in energy) of the electrons, which would allow more electrons to participate in the tunneling process at lower temperature.

At the bias of 450 mV (slightly higher than the valley-current voltage), the current increases with increasing temperature. But the temperature-dependence is not as strong as that of the thermal diffusion process. Since the barrier in the conduction band is high (1.8 eV), thermionic currents over the barrier will only give a very small current contribution. Also as indicated in Fig. 1(b), the electron tunneling process from the InAs layer is impeded by the band gap of the GaSb layer (no available states). However, in the valence band, due to a quite large band bending in the InAs layer in conjunction with its small band gap, it is possible that the light holes in the GaSb layer could easily tunnel through this potential barrier into the valence band of the InAs layer. This suggests that the hole tunneling process then is likely the dominating current transport process at the bias of 450 mV. At higher bias (500 mV), a Fowler-Nordheim-type of tunneling may begin to dominate. With an increase in the forward bias, the current is dominated by electron tunneling from the valence band of the AlSb to the unoccupied states of the valence band of the GaSb.[13]

According to the above analysis, we could suppress the valley current by growing another material, such as InAlAs, with a larger band gap than InAs on top of the InAs layer and let the InAs layer be about only 20 nm thick. In this approach, the band overlap between InAs and GaSb is maintained while the effective band gap of the n-type electrode is enlarged.

In summary we have demonstrated the room-temperature operation of the InAs/AlSb/GaSb single-barrier tunnel diode. The current transport mechanism by the interband tunneling in this structure is similar to that of a homojunction pn-tunnel diode. However, this structure eases the need for very heavy doping concentrations and offers a flexible control of the barrier thickness. In this early stage, we have obtained a peak-to-valley current ratio as high as 4.7 and a peak-current density of 3.5 kA/cm^2 at room temperature. We also studied the temperature-dependence of the current which suggests an improvement of the peak-to-valley current ratio can be achieved by using a multilayer n^+ electrode, such as InAlAs/InAs, to suppress the valley current. The device performance is expected to improve by using optimal AlSb barrier thickness.

FIG. 3. Current-Voltage characteristics as functions of temperature for five different forward biases.

[1] L. Esaki, Phys. Rev. 109, 603 (1958).
[2] L. L. Chang, L. Esaki, and R. Tsu, Appl. Phys. Lett. 24, 593 (1974).
[3] A. Y. Cho, Thin Solid Films 100, 291 (1983).
[4] T. C. L. G. Sollner, W. D. Goodhue, P. E. Tannenwald, C. D. Parker, and D. D. Peck, Appl. Phys. Lett. 43, 588 (1983).

[5] F. Capasso, S. Sen, A. Y. Cho, and D. L. Sivco, Appl. Phys. Lett. 53, 1056 (1988).

[6] L. F. Luo, R. Beresford, and W. I. Wang, Appl. Phys. Lett. 53, 2320 (1988).

[7] R. Beresford, L. F. Luo, and W. I. Wang, Appl. Phys. Lett. 55, 694 (1989).

[8] J. R. Soderstrom, D. H. Chow, and T. C. McGill, Appl. Phys. Lett. 55, 1348 (1989).

[9] J. R. Soderstrom, D. H. Chow, and T. C. McGill, Appl. Phys. Lett. 55, 1094 (1989).

[10] R. Beresford, L. F. Luo, and W. I. Wang, Appl. Phys. Lett. 54, 1899 (1989).

[11] C. Tejedor, J. M. Calleja, F. Meseguer, E. E. Mendez, C. A. Chang, and L. Esaki, Phys. Rev. B 32, 5303 (1985).

[12] L. L. Chang and L. Esaki, Surf. Sci. 98, 70 (1980).

[13] H. Takaoka, Chin-An Chang, E. E. Mendez, L. L. Chang, and L. Esaki, Physica 117B, 741 (1983).

[14] L. F. Luo, R. Beresford, and W. I. Wang, Appl. Phys. Lett. 55, 2023 (1989).

[15] L. Esaki, L. L. Chang, and E. E. Mendez, Jpn. J. Appl. Phys. 20, L529 (1981).

[16] H. Munekata, T. P. Smith, and L. L. Chang, J. Cryst. Growth 95, 235 (1989).

Photoresponse of ion-beam-deposited Y-Ba-Cu-O thin films

K. Li, R. Hsiao, and C. Tang

Boeing Aerospace and Electronics, High Technology Center, Seattle, Washington 98124-6269

We report on the microstructure and photoresponse of ion-beam-deposited Y-Ba-Cu-O granular thin films. High-temperature superconductor thin films of the average composition $YBa_{1.8}Cu_{3.6}O_x$ were ion-beam deposited onto yttria-stabilized zirconia and strontium titanate substrates from a composite target. Post-annealing processes were used to control the degree of granularity in these films, and led to films which varied in superconducting behavior. The microstructures of these films were studied by secondary electron microscopy and Auger analysis. Photoresponse and resistivity were measured as a function of temperature. We found that the degree of granularity in our films correlates with their resistivity and photoresponse which are similar to those of epitaxial or granular films.

Sensitive broadband detectors which can operate at liquid-nitrogen temperature have many technological applications, but few such detectors are available. Recent works[1-7] on thin-film superconductors have the potential to meet these requirements. In these studies, magnetron sputtering, electron beam evaporation, and laser ablation deposition were used to fabricate the thin films, and resulted in films with varying superconducting properties.

Naturally occurring grain-boundary Josephson junctions were reported[1] in low-temperature superconductor $BaPb_{0.7}Bi_{0.3}O_3$ thin films. Most of the current studies on high-temperature superconductor (HTS) Y-Ba-Cu-O thin films[2-5] were on epitaxial films which do not have grain boundaries. In another approach,[6,7] weak intergrain couplings were reported in granular Y-Ba-Cu-O thin films. The occurrence of weak links[8] in a Y-Ba-Cu-O granular film depends on its favorable microstructure for which few details have been reported.

In this communication, we looked for favorable microstructures for weak-link formations in HTS thin films with an average composition of $YBa_{1.8}Cu_{3.6}O_x$. These films were fabricated by the ion-beam-deposition approach that generically[9] was used to tailor thin films with unique properties. We used post-annealing processes to segregate the nonsuperconducting phases from the superconducting phase of the films, and this led to films varying in granu-

larity. The microstructures of these films were analyzed with scanning Auger microscopy.

Thin films used in this work were sputter deposited from a sintered oxide target[10] of composition $YBa_2Cu_{4.5}O_x$ by a Kauffman ion-beam source onto yttria-stabilized zirconia (YSZ) and strontium titanate substrates. The deposition rate was 7 nm/min. The thickness of the films was 600 nm. The argon pressure during sputtering was 9×10^{-5} Torr and the substrates were not intentionally heated during deposition. The as-deposited films were amorphorous and insulating. Their composition was $YBa_{1.8}Cu_{3.6}O_x$ as determined by inductive coupled plasma spectroscopy (ICPS)

The microstructure of $YBa_{1.8}Cu_{3.6}O_x$ thin films were changed by controlling the grain nucleation rate and grain growth rate[11] using two different post-annealing processes. In the slow growth process, films were slowly heated up in argon to 800 °C over a 50-min time period, and maintained at 800 °C in oxygen for 4 h, then slowly cooled to room temperature in 5 h. In the fast growth process, films were heated up rapidly in helium to 900 °C in 3 min, maintained at 900 °C for 10 min, and then cooled in oxygen to room temperature in 5 h. The samples were then coated with 150-nm silver contact pads, and standard four-terminal resistivity measurements were performed in a closed-cycle cryostat with windows. The photoresponse of current-